The Impact of Thermochemical Exhaust Energy Recovery Using Ethanol-Gasoline Blend on Gasoline Direct Injection Engine Performance

Mardani, Moloud; Herreros, Jose; Tsolakis, Athanasios

DOI:
10.1007/s11244-022-01757-5

Document Version
Publisher's PDF, also known as Version of record

Citation for published version (Harvard):
Mardani, M, Herreros, J & Tsolakis, A 2022, 'The Impact of Thermochemical Exhaust Energy Recovery Using Ethanol-Gasoline Blend on Gasoline Direct Injection Engine Performance', *Topics in Catalysis*.
https://doi.org/10.1007/s11244-022-01757-5

Topics in Catalysis
https://doi.org/10.1007/s11244-022-01757-5

ORIGINAL PAPER

The Impact of Thermochemical Exhaust Energy Recovery Using Ethanol-Gasoline Blend on Gasoline Direct Injection Engine Performance

Moloud Mardani[1] · **Jose Herreros**[1] · **Athanasios Tsolakis**[1]

Accepted: 24 November 2022

Abstract
Thermochemical exhaust energy recovery in a modern gasoline direct injection engine is investigated using ethanol-gasoline blend (E25) and gasoline, as base fuel. The primary objectives of this research are focused on reducing carbonaceous emissions as well as improving thermal efficiency and fuel economy in combustion engines. These are consistent with the global commitment to lessen carbon emissions and meet environmental regulations and agreements.
The possibility of hydrogen production through catalytic reforming of mentioned fuels using actual exhaust composition is investigated on full-scale Rh (Rhodium)—Pt (Platinum) catalysts. ANSYS-Chemkin is utilized for thermodynamic equilibrium analyses based on the Gibbs energy minimization method to explore the key reaction pathways for E25 reforming. Main reforming parameters including steam to carbon molar ratios and reforming temperatures are selected to investigate the feasibility of ethanol-gasoline blend reforming as well as to identify the reformate composition and evaluate the whole process efficiency. The results revealed that the presence of ethanol in reforming fuel mixture facilitates endothermic reactions and improves hydrogen-rich mixture, particularly at high engine load conditions where maximum heat recovery is obtained. Furthermore, E25 fuel reforming helped achieving up to 16% greater CO_2 compared to gasoline fuel reforming under the same engine condition. Overall, the experimental results of full-scale reforming tests using E25 can be accredited for effective implementation of the reforming technique in practical application.

Keywords Thermochemical heat recovery · Hydrogen production · Ethanol-gasoline blend · Fuel reforming · Fuel economy · CO_2 reduction

1 Introduction

In recent years, in response to the environmental effects of fossil fuels and subsequently global concerns, the consumption of renewable fuels is becoming increasingly important [1]. Hydrogen as an environmentally friendly fuel can be considered for automotive usage and has indicated benefits, especially in terms of fundamental combustion characteristics of gasoline direct injection (GDI) engines [2–5]. These include combustion stability, efficiency and knock suppression. Furthermore, combustion with H_2, as a fuel additive, leads to greater thermal efficiency, larger flammability and wider air–fuel equivalency ratio that can be tuned to lower in-cylinder temperature and the formation of NOx emissions. Ultimately, unique properties of H_2, including high octane number, high flame propagation rate and low ignition energy, contribute to improved fuel economy and reduced carbon-based particulate matter, CO and CO_2 emissions [6].

The main reactions for hydrocarbon fuel reforming are listed in Table 1. This work investigates the role of fuel composition on catalytic exhaust waste heat and species recovery via a full-scale fuel reformer coupled to a modern gasoline direct injection engine. Ethanol splash blended with ethanol as a renewable low carbon fuel is studied. Chemical equilibrium analyses were implemented to calculate the maximum possible fuel conversion reforming process and understand reaction sequences once compared to the experimental results. Reformate composition, exhaust heat and species recovery and overall reforming efficiency of E25 fuel under various reforming parameters (i.e. reactants composition,

✉ Moloud Mardani
mxm1064@bham.ac.uk

[1] Mechanical Engineering, School of Engineering, University of Birmingham, Birmingham B15 2TT, UK

Published online: 21 December 2022

Table 1 Main reforming reactions [8][26]

Reactions	Types of reaction	$\Delta H^{\circ}_{298\ k}$ (KJ/mol)
$C_8H_{18}\ (g) + 8H_2O\ (g) \rightarrow 8CO\ (g) + 17H_2\ (g)$	Isooctane steam reforming	1310
$C_2H_5OH\ (g) + H_2O\ (g) \rightarrow 2CO\ (g) + 4H_2\ (g)$	Ethanol steam reforming	256
$C_8H_{18}\ (g) + 8CO_2\ (g) \rightarrow 16CO\ (g) + 9H_2\ (g)$	Isooctane dry reforming	1639
$C_2H_5OH\ (g) + CO_2\ (g) \rightarrow 3CO\ (g) + 3H_2\ (g)$	Ethanol dry reforming	297
$C_8H_{18}\ (g) + 12.5O_2\ (g) \rightarrow 8CO_2\ (g) + 9H_2O\ (g)$	Oxidation of Isooctane	− 5065
$C_2H_5OH\ (g) + 3O_2\ (g) \rightarrow 2CO_2\ (g) + 3H_2O\ (g)$	Oxidation of ethanol	− 1366.8
$C_8H_{18}\ (g) + 4O_2\ (g) \rightarrow 8CO\ (g) + 9H_2\ (g)$	Partial oxidation of Isooctane	− 625
$2C_2H_5OH\ (g) + O_2\ (g) \rightarrow 4CO\ (g) + 6H_2\ (g)$	Partial oxidation of ethanol	43.88
$CO\ (g) + H_2O\ (g) \leftrightarrow CO_2\ (g) + H_2\ (g)$	Water–gas-shift reaction (WGS)	− 41
$CO\ (g) + 3H_2\ (g) \rightarrow CH_4\ (g) + H_2O\ (g)$	Methanation reaction I	− 206
$CO_2\ (g) + 4H_2\ (g) \leftrightarrow CH_4\ (g) + 2H_2O\ (g)$	Methanation reaction II	− 165

steam to carbon (S/C) molar ratios, fuel composition and engine operating conditions) are experimentally obtained with the aim of improving carbon footprint and fuel economy in a modern GDI engine.

In the exhaust assisted fuel reforming, waste engine exhaust gas heat can be converted to applicable chemical energy through catalyst driven endothermic reactions like steam reforming (SR) and dry reforming (DR) [7, 8. Furthermore, complete and partial oxidation reactions in presence of oxygen content in exhaust mixture generate internal heat and consequently promote the mixture temperature [9]. Available and generated heat will be absorbed by steam and dry reforming reactions, in which reforming fuel in direct contact with a stable catalyst, reacts with the engine exhaust gas CO_2 and steam, respectively, to generate H_2 and CO through various pathways [10, 11]. Exothermic feature of partial oxidation can be advantageous in fuel reforming process for vehicle applications [12].

There has been extensive research on the engine and emissions performance of renewable fuel blended with petroleum-based fuels. Due to the benefits of ethanol including renewability, oxygen content, short carbon chain and high H_2 content, it has been considered as one of the most desirable fuel extenders and fuel additives to gasoline [13]. Different gasoline-ethanol blends have been investigated in spark ignition (SI) and compression ignition (CI) engines with constant-volume combustion chambers. Overall, adopting a gasoline-ethanol splash blended in SI engines combustion causes increased engine performance, thermal efficiency, and lower emissions than gasoline fuel if an appropriate AFR (air to fuel ratio) control is applied. Moreover, because of the higher octane number of ethanol, higher compression ratios can be implemented without risk of knocking [14]. With regards to engine emissions, ethanol-gasoline blends allow performing a quicker and more effective combustion process, which grants a general decline of the THCs and CO emissions in most of the tested engines.

Ethanol properties as high hydrogen content, non-toxic, sulfur and aromatics-free represent it as one of the promising candidates for fuel reforming techniques followed by the minimum catalyst deactivation rate and surface poisoning [15].

Several reactions are involved in the overall mechanism that result in the formation of minor light hydrocarbons such as acetaldehyde and ethylene. The formation of carbonaceous accumulation on catalytically active surfaces is a critical side effect of multiple side reactions [16, 17]. Steam and auto-thermal reforming of pure ethanol has been examined experimentally and thermodynamically for different steam to fuel and oxygen to fuel molar ratios, under various ranges of temperatures and catalysts [18–20]. Low-temperature ethanol reforming has been examined using several reformer designs in which exhaust composition and heat of a light-duty vehicle were utilized to feed the reformers. The results prove that ethanol fuel reforming is beneficial in terms of fuel-saving and engine emissions reduction [21].

On-board ethanol steam reforming was investigated using exhaust gas of a GDI engine. Reforming performance as a function of temperature, reformate composition and efficiency were examined using several catalysts. Experimental assessments among the tested catalysts indicated that H_2 yield over the cobalt catalytic monolith is highly restricted by catalyst activity and coke formation, while ceria-supported Rh-Pt catalyst indicated promising performance and selectivity for H_2 production [22]. Ethanol-gasoline blend potentially limits the development of carbon zone on the catalyst surface, due to the oxygen content available in the fuel molecular structure. Moreover, considerable reactivity and diffusivity of ethanol lead to efficient use of active site of the catalyst and consequently more H_2 production. Although ethanol-gasoline blend is a potentially viable replacement for fossil fuels in combustion engines, its promising performance in terms of fuel reforming is still required to be evaluated under actual exhaust gas conditions. In recent studies, the incorporation of a prototype full-scale fuel reformer with a GDI engine is studied with gasoline fuels [23–26]. Recirculating the reformate mixture with increased calorific value back in the engine intake provides benefits in terms

of engine thermal efficiency and regulated emissions (e.g. NOx, HC) reduction.

This work investigates the role of fuel composition on catalytic exhaust waste heat and species recovery via a full-scale fuel reformer coupled to a modern gasoline direct injection engine. Ethanol splash blended with ethanol as a renewable low carbon fuel is studied. Chemical equilibrium analyses were implemented to calculate the maximum possible fuel conversion reforming process and understand reaction sequences once compared to the experimental results. Reformate composition, exhaust heat and species recovery and overall reforming efficiency of E25 fuel under various reforming parameters (i.e. reactants composition, steam to carbon (S/C) molar ratios, fuel composition and engine operating conditions) are experimentally obtained with the aim of improving carbon footprint and fuel economy in a modern GDI engine.

2 Materials and Methods

2.1 Thermodynamic Study

CHEMKIN 18.2 has been employed to perform thermodynamic equilibrium calculations. This method involves the gas-phase reaction mechanisms with consistent thermodynamic properties which could be particularly advantageous in validity of biofuels mixtures reforming process as well as estimating the reformate concentrations and process efficiency. Thermodynamic equilibrium analyses provide a comprehensive insight into the reforming process and investigate the significant effect of the main parameters including S/C molar ratios and inlet temperatures on reformate composition and temperature. Additionally, this method explains the potential reforming limitations, mechanism accuracy and facilitates experimental and theoretical comparisons. In this study, thermodynamic equilibrium calculations of ethanol and gasoline mixture were conducted based on the Gibbs free energy method for stoichiometric conditions in which S/C molar ratios ranged from 2.0 to 4.0 and operating temperatures defined from 300 to 800 °C at fixed pressure 1.0 atm. The main mechanism package consists of a combination of gas-phase reactions and thermodynamic data which have been credited by several studies and proved satisfactory agreements with target empirical results [8, 27].

2.2 Experimental Study

A modern turbocharged GDI engine with the main specifications shown in Table 2, was coupled to an AC dynamometer. The reforming behaviour of a full-scale fuel reformer, fueled with a certain volume percentage of gasoline blended with ethanol (25% ethanol and 75% gasoline) [17], under various engine operating conditions as well as fuel injection rates were studied. The characteristic of reforming fuels are indicated in Table 3. The mentioned fuel reformer injection setup contains a low-pressure fuel pump and fuel injector. A fixed fuel volume method was used to calibrate the fuel injector at a constant injection pressure of 3.0 bar. The measurements were repeated three times to minimise measurement variability and ensure repeatability. PFM (Pulse Frequency Modulation) technique, fixed turn-on-time and variable frequency were utilised to control fuel injection rates using a microcontroller. Accordingly, empirical equations of injection characteristics were gained via linear equations fitted with $R^2 > 0.99$.

Reforming tests were accomplished within five catalytic plates surrounded by a prototype fuel reformer. CZA (Ceria–Zirconia–Alumina) catalyst with coating density of 3.6 g/in^3 and loading of 3.3% Pt and 1.7% Rh is located inside the plates which were covered by stainless steel fins to maximise heat transfer [26]. Heat transfer from exhaust flow to plates delivers heat to catalytic domains to boost

Table 2 Engine specifications

Parameter	Value
Type	Four strokes
No. of Cylinders	3
Swept volume (cc)	1497
Turbocharger	RAAX turbocharger
Compression Ratio	11:1
Bore × Stroke (mm)	84 × 90
Rated Torque (Nm)	240 @ 1600–4500 rpm
Rated Power (kW)	134 @ 6000 rpm
Fuel injection system	Direct Injection (DI) and Port Fuel Injection (PFI)
Engine Management	Bosch ME0617

Table 3 Fuel properties [8]

Property	Values	
Fuel type	Gasoline	Ethanol
Molecular weight (g/mol)	83.28	46.07
Research octane number (RON)	96.8	110
Motor octane number (MON)	85.2	90
Density at 15 °C, (kg/m^3)	743.9	789
Viscosity [mm^2/s] at 40 °C	0.4–0.8	1.1
Latent heat of vaporization (kJ/kg)	350	904
Lower Heating Value LHV (kJ/kg)	42.2	26.85
Laminar flame speed (m/s)	51	63.6
Auto-ignition temperature (°C)	~300	422.8
Adiabatic flame temperature (k)	2370	2195

steam and dry reforming as highly endothermic reactions. To eliminate heat dissipation and for insulation purposes, the reformer body was enveloped using thermal insulation wrap.

FTIR (Fourier-transform Infrared Spectroscopy) MKS 2030 gas analyzer was used to record flow composition (including H_2O, CO, CO_2, CH_4, THC, etc.) before and after the reformer. HSense (V&F) was used to measure H_2 mole fraction. To minimize condensation effect of steam and hydrocarbons, the specimen was directed into the measurement devices through heating lines, held at a temperature of about 190 °C. Furthermore, Testo 340 flue gas analyser was used to measure oxygen mole fraction in exhaust composition for different engine operating conditions.

Table 4 Exhaust composition and temperature upstream the reformer

Parameter	Condition 1	Condition 2	Unit
Operating condition	35/2100	90/2500	Nm/rpm
IMEP	3.5	8.2	bar
Exhaust temperature	463	638	°C
Carbon dioxide (CO_2)	11.79	11.56	Vol.%
Carbon monoxide (CO)	6051	6257	ppm
Oxygen (O_2)	0.69	0.68	Vol.%
Water (H_2O)	12.48	12.59	Vol.%
Hydrogen (H_2)	2197	2324	ppm
Nitrogen oxides (NO_x)	1725	3043	ppm
Total hydrocarbons (THCs)	1302	1120	ppm

The engine was operated at steady-state and stoichiometric operating conditions, 35 Nm at 2100 rpm and 3.5 bar IMEP and 90 Nm at 2500 rpm and 8.2 bar IMEP. Exhaust gas composition and engine out temperature for each engine condition are reported in Table 4. The selected engine operating conditions correspond to typical engine speed and load in urban driving cycles. The operating conditions were chosen to obtain an appropriate range of temperatures (between almost 500 °C and 700 °C), exhaust flow rates and compositions for the reformer input [26].

Pelton glass tube flow meter was situated downstream of the reformer to monitor the exhaust volumetric flow rate passing through the catalytic domain. A portion of exhaust flow was captured from a low-pressure point (after the turbine) and mixed with reforming fuel. The exhaust and fuel mixture travels through a hollow space around the TWC body. The heat released by exothermic reactions inside the TWC, enables fuel evaporation and flow homogenization. The schematic of experimental setup is indicated in Fig. 1. A set of k-type thermocouples were connected to a Pico-Log data acquisition software and used for simultaneous and continuous monitoring of the temperature distribution over the middle section of the reformer. The respective position of each thermocouple is depicted in Fig. 2. Linear temperature profiles along the length of the middle plate were measured by TC 1–6, while lateral temperature variation on the surface of the catalyst was obtained by TC 7–12. Additionally, four thermocouples were placed upstream and downstream of the reformer to detect the inlet and outlet temperatures. To

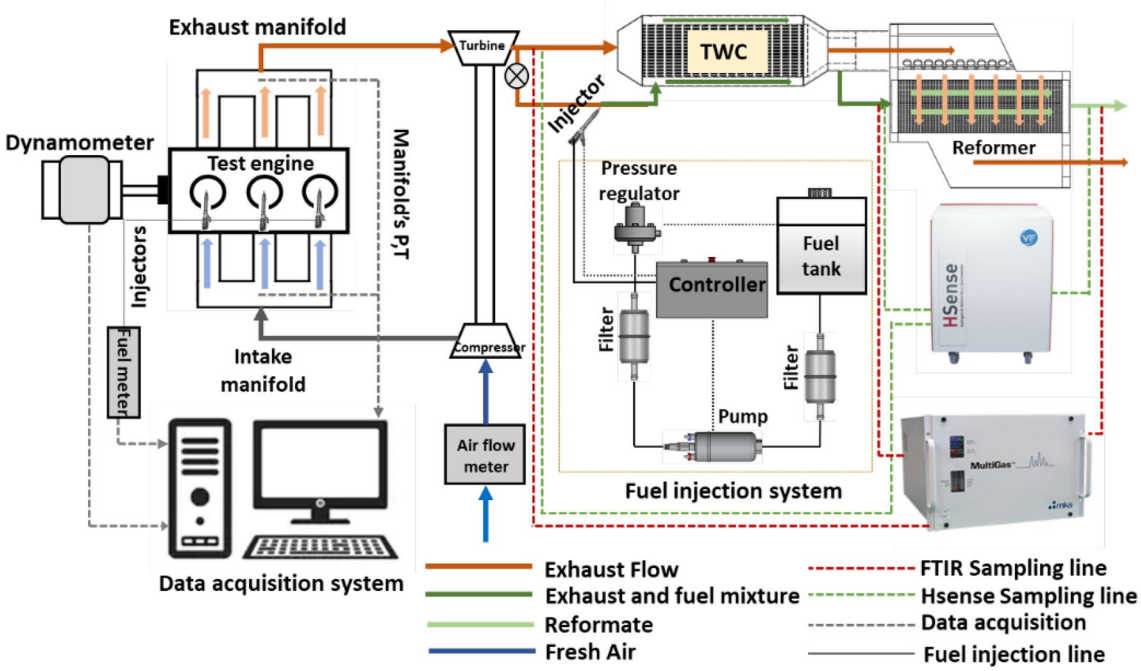

Fig. 1 Test setup

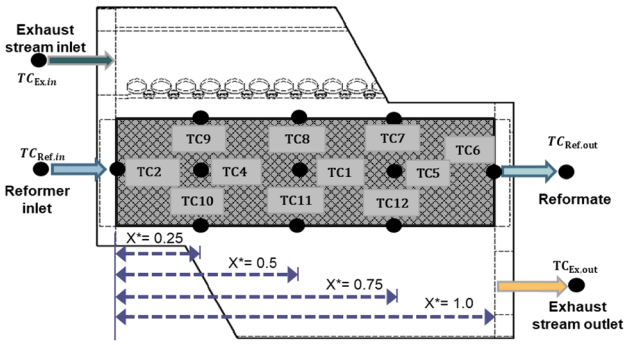

Fig. 2 Position of thermocouples in the reformer

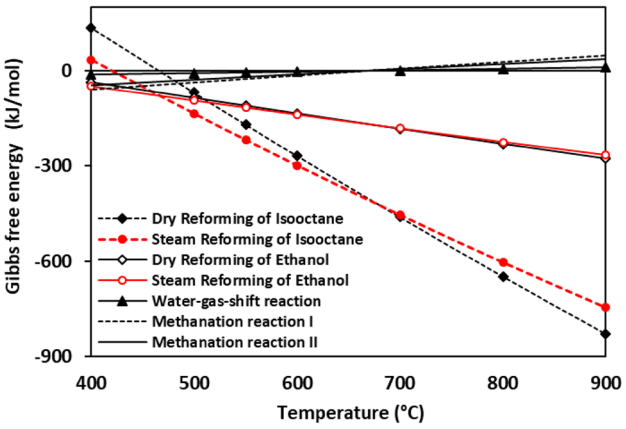

Fig. 3 Gibbs free energy of the participating reforming reactions

examine the effect of exhaust gas temperature and composition on reformate mixture and efficiency, the engine was run on two speed-load operating conditions. Furthermore, to evaluate the chemical and physical effects of reforming fuel in addition to fuel flow rate on the reforming results, the S/C molar ratio was varied from lean (S/C = 4.0) to rich (S/C = 2.0) injection rate, Table 5.

3 Results and Discussion

3.1 Equilibrium Analysis of Reforming Process

Total variation of Gibbs free energy for a system of multiple reactions is expressed based on change in enthalpy (ΔH) and entropy (ΔS) of reactants and products [28]. Hence, the values of change in Gibbs free energy (ΔG) for the main reforming reactions of ethanol and isooctane are illustrated in Fig. 3. Tendency of a reaction motivates it to reach the minimum value of change in Gibbs free energy under equilibrium conditions.

Table 5 Experimental testing conditions

Engine condition (Nm/rpm)	GHSV (1/h)	S/C	Reformer inlet temperature (°C)	Reforming fuel
Condition 1 35/2100	17,000	2	512	Gasoline
		3	520	
		4	520	
	18,000	2	496	E25
		3	497	
		4	500	
Condition 2 90/2500	18,000	2	668	Gasoline
		3	668	
		4	653	
	19,000	2	670	E25
		3	671	
		4	676	

As it is illustrated in Fig. 3, SR of isooctane and ethanol are the most dominant reactions than any other participating reactions which are in parallel with WGS, leading to higher H_2 production. However, at high catalyst inlet temperatures, DR of ethanol and isooctane are thermodynamically more favored than SR, resulting in reduction of H_2 and CO_2 concentrations and increase of CO.

The effect of catalyst inlet temperature on reformate composition using exhaust gas from a GDI engine operated under stoichiometric conditions is investigated under a fixed GHSV for S/C molar ratios varied from 2.0 to 4.0 for E25 reforming. Temperature dependency of reformate composition is illustrated in Fig. 4 using chemical equilibrium analyses. Figure 4 (a) and (b) show that H_2/CO molar ratio decreases for all S/C molar ratios at high catalyst inlet temperature.

At lower temperatures, variations of the H_2/CO_2 and H_2/H_2O ratios based on S/C molar ratios are nearly similar and the differences become more considerable when the temperature is raised. CO concentration in exhaust mixture is low and mostly produced by SR and DR reactions during the reforming process. Furthermore, temperature increment would benefit CO production where DR is favored. Also, increased fraction of H_2 production at lower temperatures indicates a growing contribution from SR, which occurs when unconverted fuel reacts with available H_2O produced by either engine or catalytic combustions. Ultimately, at high temperatures, H_2/CO molar ratio dropped steadily where H_2/CO_2 molar ratios increases simultaneously, proposing that DR reaction contributes noticeably to the conversion of reforming fuel at this stage.

3.2 Experimental Analysis of the Reforming Process

3.2.1 Reformate Composition

Figure 5 demonstrates the reformate composition as a function of reformer inlet temperature for a constant S/C molar

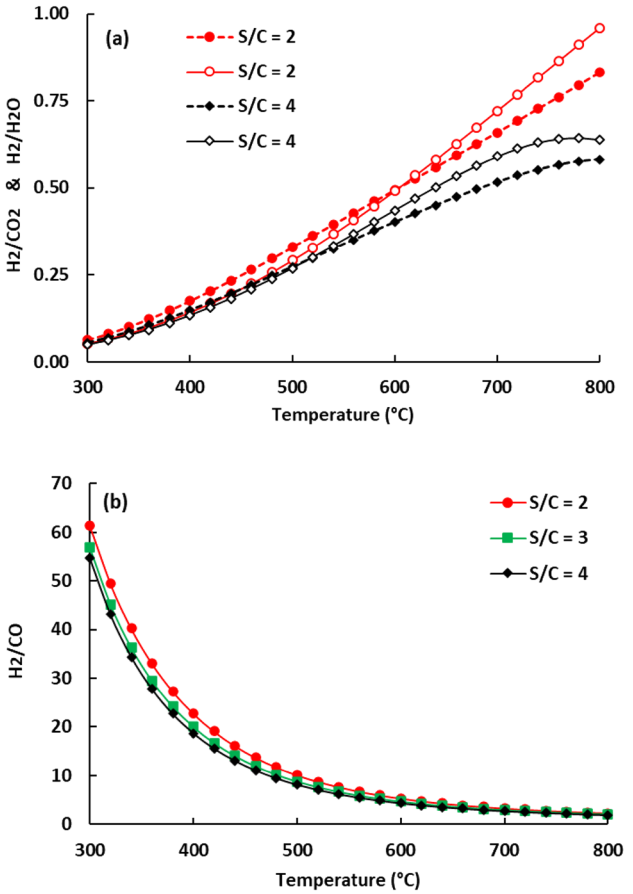

Fig. 4 **a** H_2/H_2O (solid lines) and H_2/CO_2 (dashed lines) as a function of catalyst inlet temperature for S/C = 2 and 4 and **b** H_2/CO as a function of catalyst inlet temperature for S/C = 2 to 4, at fixed GHSV ~ 17,000 1/h and pressure 1.0 atm

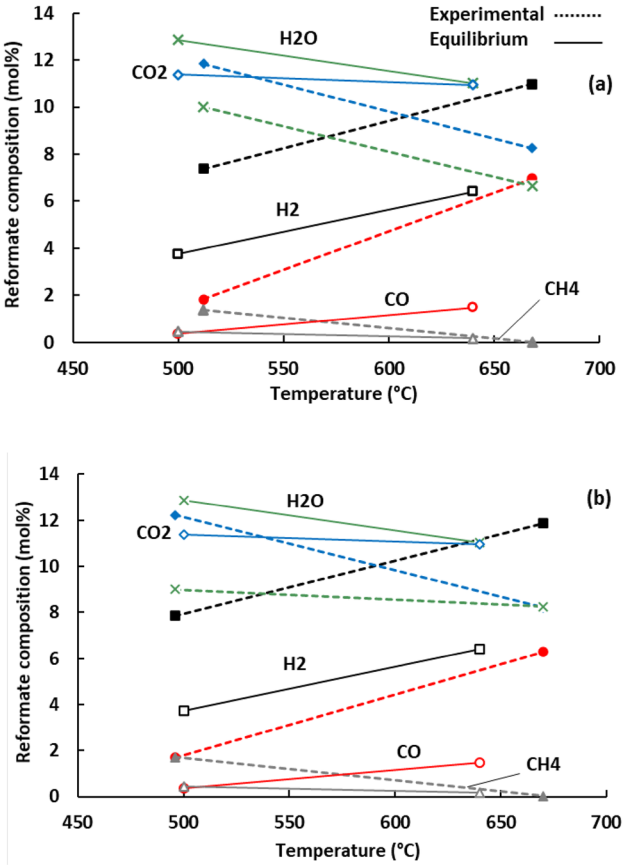

Fig. 5 Reformate composition as a function of temperature at GHSV ~ 17,000 1/h, S/C 2.0 for **a** Gasoline and **b** E25

ratio of 2.0 based on experimental analyses. The results confirm that experimental trends for both fuels and engine conditions are in agreement with equilibrium results. Figure 5 (a) and (b) experimentally confirm that H_2 production from E25 reforming is higher than in the case of pure gasoline reforming. It is because of that gasoline SR and DR are more endothermic in comparison to ethanol reforming reactions. Therefore, compared to gasoline, SR and DR of ethanol are more feasible, as it has weaker molecular bonds which makes it more feasible to reform [8].

Variation in reformate products (shown in Fig. 5) can be explained based on reforming reaction sequences as a function of inlet temperature. SR and DR reactions in addition to WGS are the three main reactions for H_2 production. At low catalyst inlet temperature (engine operating condition 1), SR (less energy required to support SR with respect to DR) is the main reaction for H_2 and CO production hence H_2O consumption. While, at high reforming temperature (engine operating condition 2) endothermic reactions are more likely, and DR takes over SR, Fig. 3. Moreover, high operational temperature reduces the WGS reaction rate promoting inverse WGS, leading to more CO production and lower H_2/CO molar ratios. H_2O concentration is mainly controlled by SR and WGS reactions during the reforming process. The minimum value is obtained at engine condition 2 where SR and WGS move in the same direction toward H_2 production and H_2O consumption. H_2O mole fraction obtained from E25 reforming is lower than pure gasoline which is evidence that SR of ethanol is more favored. As the temperature of the reforming mixture increases, the amount of CH_4 in the mixture declines (increase H_2/CH_4 molar ratios). In this case, methanation reactions at high temperatures lead to CH_4 conversion rather than CH_4 production.

Hydrogen production as a function of CO_2, CO, H_2O and CH_4 is shown in Fig. 6 based on S/C molar ratios at engine operating condition 2. For a fixed steam concentration in exhaust mixture, increasing fuel injection (reducing S/C molar ratios) favors H_2 production. At higher inlet temperatures (condition 2) DR is more favorable which boosts CO_2 consumption and H_2 and CO production rate simultaneously, Fig. 5.

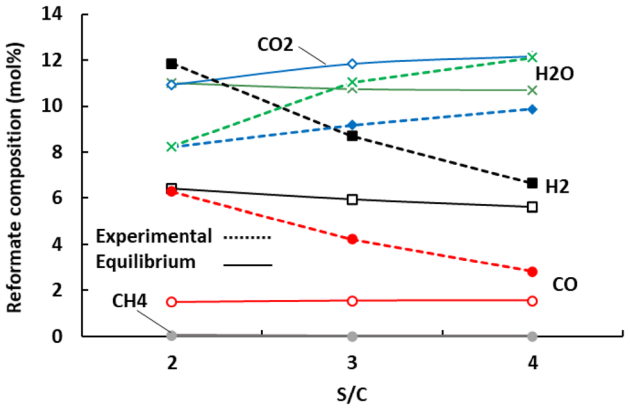

Fig. 6 Reformate composition as a function of S/C molar ratio at GHSV ~ 17,000 1/h and engine condition 2 for E25

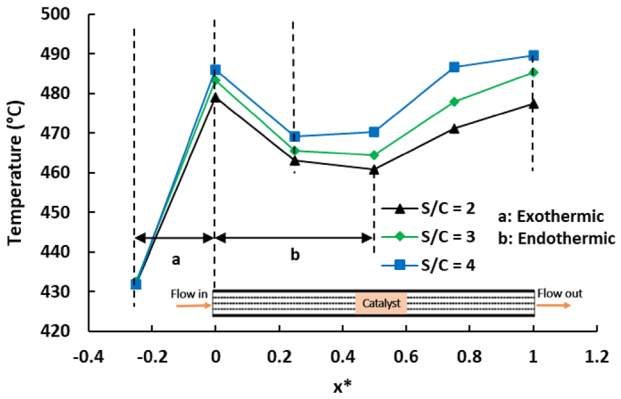

Fig. 8 Temperature distribution for Gasoline and E25 and S/C 2.0 and 4.0, GHSV ~ 17,000 1/h and engine condition 1

3.2.2 Reformer Temperature Distribution

Additional understanding of the reforming process inside the catalytic domain can be achieved from temperature profile analyses inside the plates. Linear temperature distributions inside the middle plate at engine operating condition of 35/2100 Nm/rpm and S/C molar ratios ranging from 2.0 to 4.0 are demonstrated in Figs. 7 and 8. Exhaust gas space velocity is considered constant, approximately 17,000 1/h, for all the reforming tests.

High temperature zones can be clearly observed in the front of the catalyst as a result of exothermic oxidation reactions corresponding to feed fuel and oxygen content available in the reactants. As it is shown in Fig. 8, temperature increment is more intense for S/C ratios of 4.0 and for gasoline fuel which has a greater heat release rate and lower heat of vaporisation than ethanol. The entrance temperature is lower for the S/C molar ratio of 2.0 because more fuel injection before the reformer leads to a slight temperature drop as a result of fuel vaporisation.

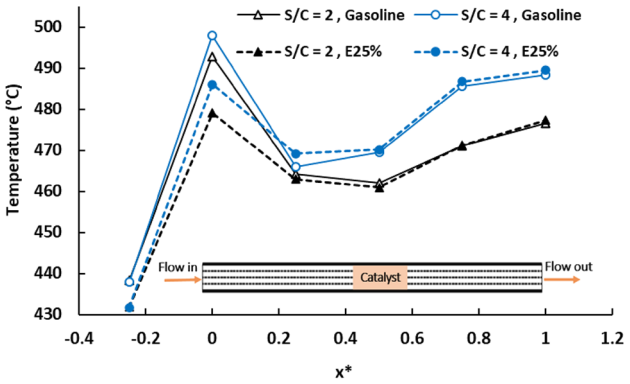

Fig. 7 Temperature distribution as a function of S/C molar ratios for fixed GHSV ~ 17,000 1/h and engine condition 1, reforming fuel E25

Subsequently, the main part of the catalytic reaction cycle starts with highly endothermic reactions (SR and DR) resulting in a gradual temperature drop by almost the middle of the plate. The majority of H_2 species is produced in this area. Endothermic zone for E25 reforming is wider compared to gasoline supporting the higher H_2 production associated with less endothermicity of ethanol SR and DR than gasoline reforming.

When the amount of fuel injection increases (S/C = 2.0) the active site of the catalyst will be occupied by extra fuel. Consequently, availability of space for fuel adsorption on the catalyst surface becomes competitive, hence the longer length of the catalyst is utilised to drive the main reforming reactions, as shown in Fig. 8. From the middle of the catalyst length, temperature profiles move upward increasingly due to external heat transfer from the main exhaust flow which passes over the finned plates.

Two-dimensional temperature distributions over the middle plate are illustrated in Fig. 9 for engine conditions 35/2100 and 90/2500 Nm/rpm and two fuel injection rates (S/C of 2.0 and 4.0). Based on thermocouples positions, Fig. 2, exhaust and fuel mixture enters at the bottom and moves upward. Furthermore, the external main exhaust flow passes through fins from right to left leading to a hotter zone across the right border. Comparing the baseline plots, Fig. 9 (a-i) and (b-i) in both engine conditions, at high condition (condition2) the reforming plates are warmed more efficiently and uniformly. For both engine conditions and S/C molar ratios, in the front zone, temperature is higher than the middle zone due to oxidation process of fed fuel. Afterward, temperature profiles cool down followed by endothermic reactions in addition to convection cooling effect of the stream. It is also clear from the plots in Fig. 9 that for higher fuel injection rate (S/C = 2.0) temperature distribution decreased slightly as

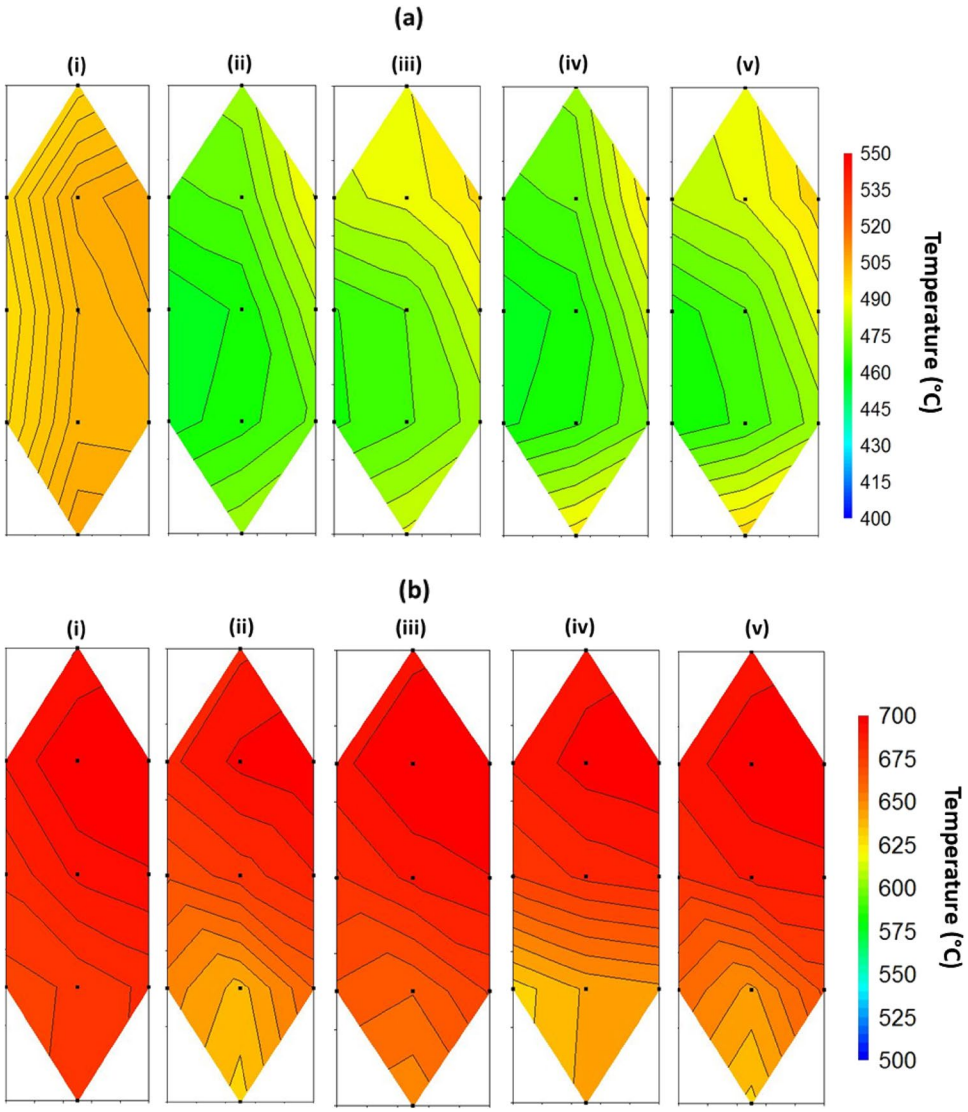

Fig. 9 **a** Engine condition 35/2100 Nm/rpm (i) Baseline (ii) E25 S/C 2.0, (iii) E25 S/C 4.0, (iv) Gasoline S/C 2.0, (v) Gasoline S/C 4.0, **b** Engine condition 90/2500 Nm/rpm (i) Baseline (ii) E25 S/C 2.0, (iii) E25 S/C 4.0, (iv) Gasoline S/C 2.0, (v) Gasoline S/C 4.0

a result of fuel vaporization and competition for active site of the catalyst which leads to a longer endothermic area.

3.2.3 Reforming Efficiency

The efficiency of the reforming process for both fuels, engine operating conditions and S/C molar ratios is determined by Eq. 1. The S/C molar ratios are adjusted from 2.0 to 4.0 and calculations are carried out based on experimental reformate compositions for both reforming fuels, E25 and gasoline. LHV fuel prod and LHV fuel refer to lower heating value of combustible contents in reactor outlet and inlet respectively [29]. The energy content of combustible gas species in the feed exhaust flow is not considered. It is therefore possible for reforming efficiency to exceed 100%, suggesting that the process is endothermic and heat recovery was successful [8]. It is worth noting that THCs available in reformate syngas provide positive contributions to reforming efficiency as they are containing chemical energy.

$$Reforming\ efficiency_{H_2\&CO}(\%) = \frac{LHV_{fuel\ products}\,\dot{m}_{fuel\ products}}{LHV_{fuel\ inlet}\,\dot{m}_{fuel\ inlet}} \times 100 \quad (1)$$

As it is indicated in Fig. 10, temperature is a beneficial parameter on overall efficiency. Referring to Eq. (1), the efficiency of a reforming process is directly associated with H_2 and CO concentrations in the reformate mixture, while it is inversely related to fuel injection flow rate. Hence, increasing the S/C molar ratio and subsequently decreasing the fuel flow rate (for a fixed amount of steam) can positively impact the efficiency rate. Equation 1 is used to verify the contribution of H_2 species in process efficiency indicating that at low engine operating conditions (lower temperature) H_2 has a stronger impact on efficiency ratings.

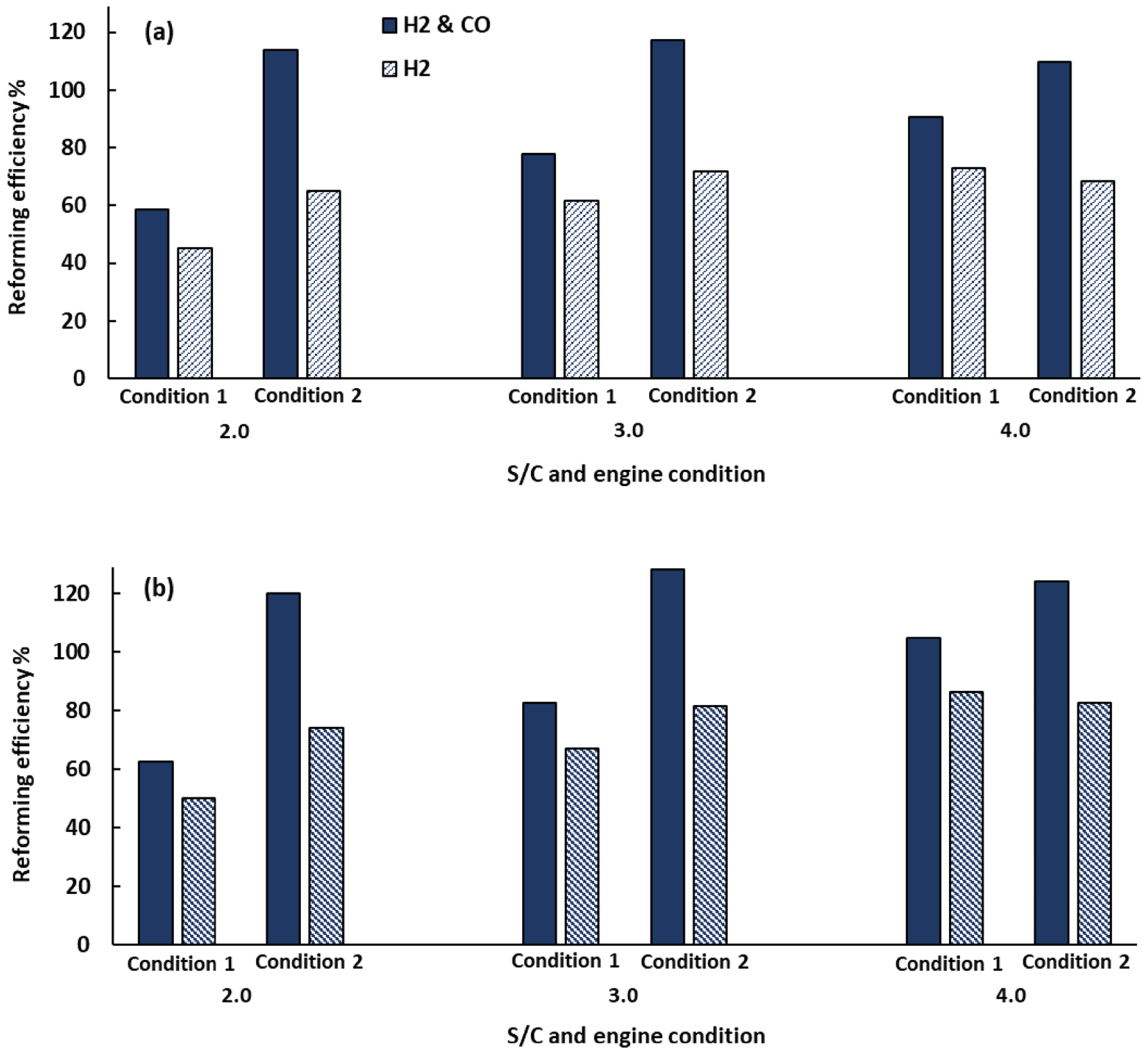

Fig. 10 Reforming process efficiency as a function of S/C molar ratio and engine condition **a** Gasoline **b** E25

3.2.4 CO_2 Reduction and Fuel Saving

The potential CO_2 reduction and fuel saving were calculated theoretically and assumed the obtained reformate was fed back to the engine's intake manifold as REGR (reformed exhaust gas recirculation). CO_2 emission of GDI engine (with gasoline fuel only) was compared against the same engine condition using reformate to partially replace an equivalent amount of gasoline energy under similar GHSV, assuming all combustible components (H_2, CO, THCs) will be converted into energy. The outcomes are depicted in Figs. 11 and 12. The overall results confirm that REGR technique is advantageous in terms of both improving carbon emissions and fuel economy with respect to the same GDI engine operating at the same engine conditions.

In this study, C–H–O–N (carbon, hydrogen, oxygen, and nitrogen) fuel combustion equation was utilised to calculate CO_2 emissions at the same engine operating conditions

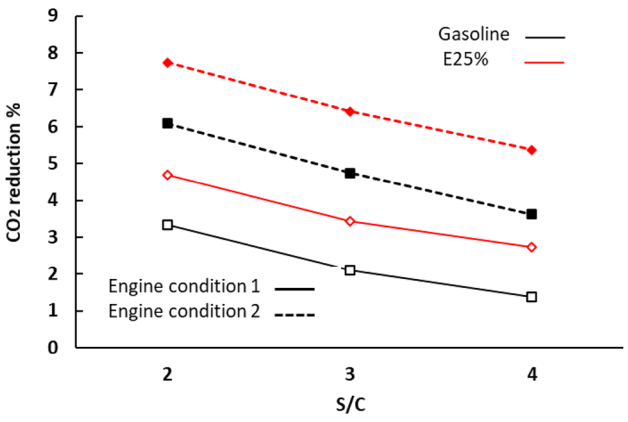

Fig. 11 CO_2 reduction% as a function of S/C molar ratio and engine condition at GHSV ~ 17,000 1/h for both reforming fuels (Gasoline and E25),

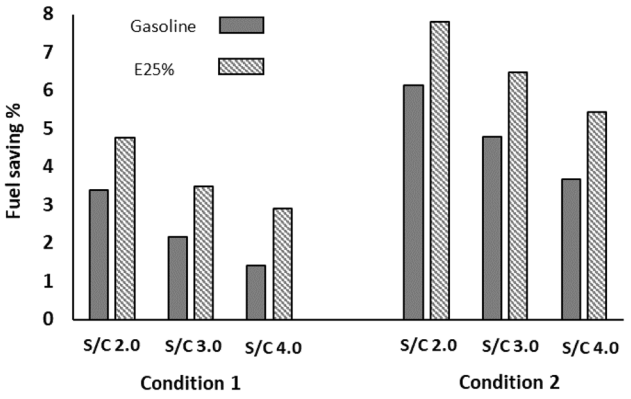

Fig. 12 Fuel saving% as a function of S/C molar ratio and engine condition at GHSV ~ 17,000 1/h for both reforming fuels (Gasoline and E25)

when the engine is fueled just by gasoline and assuming the reformate (H_2, CO, hydrocarbon species) is introduced in the engine intake. In this case, it was assumed that the same brake thermal efficiency (η_{th}) when the engine is fueled by gasoline and by the reformate. However, using H_2-rich gas will improve the η_{th} [24], however constant η_{th} was assumed for simplicity. It is worth emphasizing that there are other combustible species in the reformer feed gas and unburnt combustion products (e.g. hydrocarbon species) that are taken into account to calculate fuel and CO_2 savings. The presence of those combustible species positively affects the overall increase in LHV of the reformate and thus contributing fuel and CO_2 savings.

The CO_2 reductions and fuel-savings present an inverse relation to S/C molar ratio and direct relation to reforming temperature for both fuels. For a constant steam concentration, more fuel supply at reforming inlet benefits endothermic reactions which subsequently facilitates H_2 production and enhances reformate calorific value. Furthermore, at higher engine operating conditions and hence elevated reforming temperatures, substantial thermal efficiency and energy recovery are predicted as a result of efficient fuel reforming and H_2 production, leading to more stable and fuel-efficient combustion.

Reductions in fuel consumption and CO_2 in presence of H_2 and CO in the reformer products positively impact fuel economy and reduces CO_2 emissions, simultaneously. As it is shown in Fig. 11, this advantage is more pronounced for E25 at high load operating conditions, condition 2, in which the maximum CO_2 reduction of nearly 7.75% can be achieved at S/C molar ratio of 2.0. This variation is attributed to the more effective process efficiency and higher calorific value of the reformate mixture for E25 reforming compared to the gasoline reforming process.

Figure 12 indicates that under the investigated S/C molar ratios and temperatures, the fuel reforming technique would offer fuel savings, which is consistent with the CO_2 reduction graph, Fig. 11. The maximum fuel-saving, almost 7.80%, can be achieved for E25 at engine condition 2 and S/C of 2.0. In this case, more fuel injection in the reformer (S/C = 2.0) for a fixed steam concentration, enhances CO and H_2 in the reformate mixture. These improvements are sufficient to promote the reformate enthalpy and therefore energy replacement and fuel economy.

Overall, the maximum achievable CO_2 reduction and fuel saving from E25 reforming are approximately 16% greater than pure gasoline. It is worth mentioning that in real application of a full-scale fuel reformer in exhaust infrastructure and parallel application with a GDI engine, greater fuel economy and CO_2 reduction can be obtained as a result of more efficient fuel reforming and greater H_2 production which leads to more stable and fuel-efficient combustion.

4 Conclusions

In this study, the impact of ethanol addition to gasoline (E25) on the overall reforming process and hence engine exhaust gas heat recovery were evaluated experimentally and analytically. H_2 production and reforming efficiency were investigated in a full-scale exhaust gas fuel reformer, coupled with a modern GDI engine with the main aim of further CO_2 reduction and fuel-saving in comparison to when gasoline was utilized as reforming fuel. Using gasoline or E25, as reforming fuel, confirms that recirculating the reformate mixture to the engine intake and then partial replacement of the engine fuel energy with increased calorific value mixture is applicable and beneficial in terms of engine thermal efficiency and emissions reduction. The intensity of the main reforming reaction mechanism as well as reaction sequences highly depends on various reforming parameters including reactants composition, S/C molar ratios, fuel composition and engine operating conditions.

Chemical equilibrium analyses are in acceptable agreement with experimental data and prove that E25 is a promising fuel for on-board H_2 production. As a result of specific physical and chemical properties of ethanol, greater waste exhaust heat recovery can be achieved using an ethanol-gasoline blend which benefits H_2 and CO yield. It is also observed that the reforming performance substantially depends on both S/C molar ratios and engine operating conditions. In terms of fuel replacement, gasoline needs a higher reforming temperature than E25 to offer comparable H_2 production and conversion efficiency. In this case, the maximum process efficiency of ~ 130% and maximum fuel saving of about 8% corresponding to E25 input fuel are obtained at high load condition and S/C ratio of 3.0.

Considering steady-state stoichiometric engine operating conditions, E25 suggests maximum CO_2 reduction and fuel

saving of nearly 7.75% and 7.80%, respectively, at S/C molar ratio of 2.0, which is 16% greater than pure gasoline for both CO_2 reduction and fuel saving. This variation is attributed to the more effective process efficiency and higher calorific value of the reformate mixture for E25 reforming compared to the gasoline reforming process.

Acknowledgements Moloud Mardani would like to thank the University of Birmingham for her scholarship. EPSRC (EP/P03117X/1) is acknowledged for supporting this work and Johnson Matthey for providing the catalysts.

Data availability The data that support the findings of this study are available from the corresponding author, [Moloud Mardani],upon request.

Declarations

Conflict of interest The authors declare that they have no known competing financial interests or personal relationships that could have appeared to influence the work reported in this paper.

References

1. Granovskii M, Dincer I, Rosen MA (2007) Exergetic life cycle assessment of hydrogen production from renewables. J Power Sources 167:461–471
2. Yu X, Li D, Yang S, Sun P, Guo Z, Yang H, Li Y, Wang T (2020) Effects of hydrogen direct injection on combustion and emission characteristics of a hydrogen/Acetone-Butanol-Ethanol dual-fuel spark ignition engine under lean-burn conditions. Int J Hydrogen Energy 45:34193–34203
3. Kim J, Chun KM, Song S, Baek HK, Lee SW (2020) Improving the thermal efficiency of a T-GDI engine using hydrogen from combined steam and partial oxidation exhaust gas reforming of gasoline under low-load stoichiometric conditions. Fuel 273:117754
4. Du Y, Yu X, Liu L, Li R, Zuo X, Sun Y (2017) Effect of addition of hydrogen and exhaust gas recirculation on characteristics of hydrogen gasoline engine. Int J Hydrogen Energy 42:8288–8298
5. Naruke M, Morie K, Sakaida S, Tanaka K, Konno M (2019) Effects of hydrogen addition on engine performance in a spark ignition engine with a high compression ratio under lean burn conditions. Int J Hydrogen Energy 44:15565–15574
6. Wang S, Ji C, Zhang M, Zhang B (2010) Reducing the idle speed of a spark-ignited gasoline engine with hydrogen addition. Int J Hydrogen Energy 35:10580–10588
7. Tsolakis A, Megaritis A (2005) Partially premixed charge compression ignition engine with on-board H2 production by exhaust gas fuel reforming of diesel and biodiesel. Int J Hydrogen Energy 30:731–745
8. Mardani M, Tsolakis A, Nozari H, Martin Herreros J, Wahbi A, Sittichompoo S (2021) Synergies in renewable fuels and exhaust heat thermochemical recovery in low carbon vehicles. Appl Energy 302:117491
9. Brookshear DW, Pihl JA, Szybist JP (2018) Catalytic steam and partial oxidation reforming of liquid fuels for application in improving the efficiency of internal combustion engines. Energy Fuels 32:2267–2281
10. Liao C-H, Horng R-F (2016) Investigation on the hydrogen production by methanol steam reforming with engine exhaust heat recovery strategy. Int J Hydrogen Energy 41:4957–4968
11. Song C (2002) Fuel processing for low-temperature and high-temperature fuel cells: Challenges, and opportunities for sustainable development in the 21st century. Catal Today 77:17–49
12. Hohn KL, Schmidt LD (2001) Partial oxidation of methane to syngas at high space velocities over Rh-coated spheres. Appl Catal A Gen 211:53–68
13. Selvan VAM, Anand RB, Udayakumar M (2009) Effects of cerium oxide nanoparticle addition in diesel and diesel-biodiesel-ethanol blends on the performance and emission characteristics of a CI engine. J Eng Appl Sci 4:1819–6608
14. Koç M, Sekmen Y, Topgül T, Yücesu HS (2009) The effects of ethanol–unleaded gasoline blends on engine performance and exhaust emissions in a spark-ignition engine. Renew Energy 34:2101–2106
15. Arku P, Regmi B, Dutta A (2018) A review of catalytic partial oxidation of fossil fuels and biofuels: Recent advances in catalyst development and kinetic modelling. Chem Eng Res Des 136:385–402
16. Auprêtre F, Descorme C, Duprez D (2002) Bio-ethanol catalytic steam reforming over supported metal catalysts. Catal Commun 3:263–267
17. Hergueta C, Tsolakis A, Herreros JM, Bogarra M, Price E, Simmance K, York APE, Thompsett D (2018) Impact of bio-alcohol fuels combustion on particulate matter morphology from efficient gasoline direct injection engines. Appl Energy 230:794–802
18. da Silva AM, de Souza KR, Jacobs G, Graham UM, Davis BH, Mattos LV, Noronha FB (2011) Steam and CO2 reforming of ethanol over Rh/CeO2 catalyst. Appl Catal B Environ 102:94–109
19. Chen CC, Tseng HH, Lin YL, Chen WH (2017) Hydrogen production and carbon dioxide enrichment from ethanol steam reforming followed by water gas shift reaction. J Clean Prod 162:1430–1441
20. Lima da Silva A, de Malfatti C, F and Müller I L, (2009) Thermodynamic analysis of ethanol steam reforming using Gibbs energy minimization method: A detailed study of the conditions of carbon deposition. Int J Hydrogen Energy 34:4321–4330
21. Sall ED, Morgenstern DA, Fornango JP, Taylor JW, Chomic N, Wheeler J (2013) Reforming of ethanol with exhaust heat at automotive scale. Energy Fuels 27:5579–5588
22. Casanovas A, Divins NJ, Rejas A, Bosch R, Llorca J (2017) Finding a suitable catalyst for on-board ethanol reforming using exhaust heat from an internal combustion engine. Int J Hydrogen Energy 42:13681–13690
23. Bogarra M, Herreros JM, Tsolakis A, York APE, Millington PJ, Martos FJ (2017) Impact of exhaust gas fuel reforming and exhaust gas recirculation on particulate matter morphology in Gasoline Direct Injection Engine. J Aerosol Sci 103:1–14
24. Fennell D, Herreros J, Tsolakis A (2014) Improving gasoline direct injection (GDI) engine efficiency and emissions with

hydrogen from exhaust gas fuel reforming. Int J Hydrogen Energy 39:5153–5162
25. Bogarra M, Herreros JM, Tsolakis A, York APE, Millington PJ (2016) Study of particulate matter and gaseous emissions in gasoline direct injection engine using on-board exhaust gas fuel reforming. Appl Energy 180:245–255
26. Fennell D, Herreros J, Tsolakis A, Cockle K, Pignon J and Millington P 2015 Thermochemical recovery technology for improved modern engine fuel economy-part 1: Analysis of a prototype exhaust gas fuel reformer *RSC Adv.* **5** 35252–61
27. Mehl M, Curran H J, Pitz W J and Westbrook C K (2009) *Chemical kinetic modeling of component mixtures relevant to gasoline*. Lawrence Livermore National Lab(LLNL), Livermore, CA (United States)
28. Katiyar N, Kumar S, Kumar S (2013) Comparative thermodynamic analysis of adsorption, membrane and adsorption-membrane hybrid reactor systems for methanol steam reforming. Int J Hydrogen Energy 38:1363–1375
29. Ahmed S, Krumpelt M (2001) Hydrogen from hydrocarbon fuels for fuel cells. Int J Hydrogen Energy 26:291–301